Available online at www.sciencedirect.com
ScienceDirect
Journal of Sound and Vibration 315 (2008) 641–663
JOURNAL OF SOUND AND VIBRATION
www.elsevier.com/locate/jsvi

Low-dimensional models for the nonlinear vibration analysis of cylindrical shells based on a perturbation procedure and proper orthogonal decomposition

P.B. Gonçalves[a,*], F.M.A. Silva[a], Z.J.G.N. Del Prado[b]

[a]*Civil Engineering Department, Pontifical Catholic University, PUC-Rio, 22451-900 Rio de Janeiro, RJ, Brazil*
[b]*Civil Engineering Department, Federal University of Goiás, UFG, 74605-220 Goiânia, GO, Brazil*

Accepted 30 January 2008
The peer review of this article was organised by the Guest Editor
Available online 28 March 2008

Abstract

In formulating mathematical models for dynamical systems, obtaining a high degree of qualitative correctness (i.e. predictive capability) may not be the only objective. The model must be useful for its intended application, and models of reduced complexity are attractive in many cases where time-consuming numerical procedures are required. This paper discusses the derivation of discrete low-dimensional models for the nonlinear vibration analysis of thin cylindrical shells. In order to understand the peculiarities inherent to this class of structural problems, the nonlinear vibrations and dynamic stability of a circular cylindrical shell subjected to static and dynamic loads are analyzed. This choice is based on the fact that cylindrical shells exhibit a highly nonlinear behavior under both static and dynamic loads. Geometric nonlinearities due to finite-amplitude shell motions are considered by using Donnell's nonlinear shallow-shell theory. A perturbation procedure, validated in previous studies, is used to derive a general expression for the nonlinear vibration modes and the discretized equations of motion are obtained by the Galerkin method using modal expansions for the displacements that satisfy all the relevant boundary and symmetry conditions. Next, the model is analyzed via the Karhunen–Loève expansion to investigate the relative importance of each mode obtained by the perturbation solution on the nonlinear response and total energy of the system. The responses of several low-dimensional models are compared. It is shown that rather low-dimensional but properly selected models can describe with good accuracy the response of the shell up to very large vibration amplitudes.

1. Introduction

Thin-walled cylindrical shells are one of the most common structural elements with applications in nearly all engineering fields. Also, their static and dynamic behavior has been continuously studied since the early twentieth century. In spite of this continuous interest, several aspects of their behavior are not well understood. Among these topics, the nonlinear dynamic behavior of cylindrical shell is still an active research

*Corresponding author. Tel.: +55 21 3527 1188; fax: +55 21 3527 1195.
E-mail address: paulo@puc-rio.br (P.B. Gonçalves).

0022-460X/$ - see front matter © 2008 Elsevier Ltd. All rights reserved.
doi:10.1016/j.jsv.2008.01.063

area in applied mechanics and engineering design. The study of the nonlinear vibrations of cylindrical shells began in the middle of the last century with the works by Chu [1], Evensen [2], Dowell and Ventres [3], Atluri [4], Chen and Babcock [5] and Ginsberg [6], among others. A detailed review of this subject, including more than 350 papers, was published in 2003 by Amabili and Païdoussis [7]. Another review paper, including relevant contributions from Eastern Europe, was published in 1998 by Kubenko and Koval'chuk [8]. However, only in recent years, due to the advances in theoretical and numerical tools in the field of nonlinear dynamics, the complex nonlinear vibrations and bifurcations of cylindrical shells under various loading conditions began to be understood.

To capture the nonlinear response of cylindrical shells, large numerical models are usually employed. These analyses involving a large number of degrees of freedom are very expensive with respect to both storage and CPU time. As a result, it is difficult, if not impossible, to deal with a number of situations such as: continuation or homotopy methods for computing state solutions, in particular bifurcation diagrams under dynamic loads, evolution and erosion of basins of attraction, feedback control, parametric studies of state solutions and stability boundaries in control space. An attractive alternative is to derive consistent reduced-order models that can capture the main characteristics of the shell behavior.

Recently, a lot of attention has been paid to reducing the cost of the nonlinear state solution by using reduced-order models for the state. Particularly in solid and fluid mechanics this has become a very attractive research field, enabling a deeper understanding of complex nonlinear systems. The most common approaches are the use of nonlinear normal modes [9], which is based on the method of normal forms [10], proper orthogonal decomposition based on Karhunen–Loève method [11] and centroidal Voronoi tessellations [12]. Recently, Rega and Troger [13], in an article that introduces a special issue of the journal Nonlinear Dynamics on reduced-order models have analyzed the most common methods of dimension reduction in nonlinear dynamics with emphasis on applications in mechanics. The aim of these methods is to choose a reduced basis $\mathbf{u}_i$, $i = 1,\ldots,n$, where n is small compared to the usual number of functions used, for example, in a finite element approximation or in a traditional Galerkin model. It is clear that the reduced basis should be chosen so that it contains all the features, e.g., the dynamics of the states encountered during the simulation. It requires some intuition about the states to be simulated. If the reduced-order model is properly selected, it should work in an interpolatory setting, but it is not clear what happens in an extrapolatory setting. One cannot hope to determine one reduced-order model capable of describing the response of a complex system for all sets of parameters. So, depending on the complexity of the systems, various reduced-order models optimized for different sets of parameters should be derived. However, one hopes that a single reduced basis can be used for several state simulations or in several design settings.

Traditionally, low order models have been used to study the nonlinear vibrations of cylindrical shells. Evensen [14] proposed a reduced-order model, considering both the basic linear vibration mode plus an axi-symmetric mode, which described qualitatively the expected softening behavior of the shell observed in experiments [15]. Later, Croll and Batista [16] and Hunt et al. [17], among others, have shown that these modes are also essential for the correct description of the softening post-buckling path of cylindrical shells, being responsible for the dominant quadratic nonlinearities in the discretized equations obtained by a traditional Galerkin or Ritz approach. The essential modes to describe the nonlinear behavior of an infinitely long cylindrical shell were derived by Gonçalves and Batista [18], using a perturbation procedure, and a reduced model, based on this general solution, was adopted to study the nonlinear vibration of a simply supported, fluid-filled cylindrical shell. Recently, Gonçalves and Del Prado [19,20] used this modal expansion of the nonlinear displacement field to study the convergence of bifurcation diagrams, orbits in the n-dimensional phase space and Poincaré maps up to very large deflections, identifying the relative importance of the modes in the nonlinear analysis. Amabili et al. in a series of paper (see, for example, Refs. [21,22]), have used a modal expansion composed of two trigonometric series to study several aspects of the nonlinear dynamic response of empty and fluid-filled cylindrical shells, one containing axially asymmetric modes and the other a series of axi-symmetric modes, capturing in this way the basic nonlinear modal interactions. Based on this general solution, several reduced-order models were derived. Low order models have also been used by Popov [23] and Jansen [24] to study the nonlinear vibrations of cylindrical shells.

Modal solutions used in traditional Galerkin or Ritz procedures may attain convergence up to very large deflections using a rather large number of modes. However, this may contain redundant information in the

sense that the dynamics of the shell can be well approximated by a set of functions of much lower dimension. So, the problem is to extract a reduced basis of smaller dimension that contains all the essential information of the basis of larger dimension. One promising way is the use of the proper orthogonal decomposition based on the Karhunen–Loève method. It uses a series of snapshots of the phase space, obtained by numerical simulation using a high-fidelity model or from experiments, in order to build the reduced subspace. The method furnishes the best linear orthogonal basis, which decorrelates the signal components and maximizes variance. This method was used by Amabili et al. [25,26] to study the nonlinear vibrations of cylindrical shells. Recently, Amabili and Touzé [27,28] compared the efficiency of the proper orthogonal decomposition and the nonlinear normal modes method to build reduced-order models of a water-filled cylindrical shell. They point out the merits of each approach and conclude that for very large vibration amplitudes and a large range of parameter variations, the proper orthogonal decomposition (POD) method performs better due to its global nature.

In this paper an alternative procedure is used to obtain a precise solution for the nonlinear response of a cylindrical shell, satisfying exactly the in-plane equilibrium equations and all the relevant boundary, continuity and symmetry conditions. Based on this formulation, a low-dimensional model is derived by the use of perturbation techniques together with the proper orthogonal decomposition procedure. The free and forced response is analyzed. The results show that rather low-dimensional models can be employed to study the response of the shell up to very large deflections. The present methodology, combining a perturbation procedure with POD, can be easily extended to a series of structural elements such as beams, arches and plates and other shell geometries. Once the linear vibration modes are obtained, the higher-order modes can be derived by the perturbation procedure and, then, the POD method can be used to select the most important modes.

2. Formulation of the problem

Consider a thin-walled, simply supported cylindrical shell of radius R, length L and thickness h. A cylindrical coordinate system is adopted with the center at the lower end of the shell, as illustrated in Fig. 1. The mid-surface displacements in the axial, circumferential and radial directions are denoted, respectively, by u, v and w. The shell material is considered to be elastic, homogeneous and isotropic with Young's modulus E, Poisson ratio ν and density ρ.

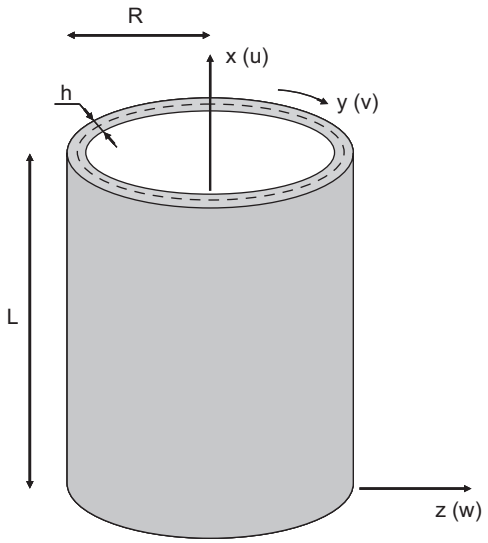

Fig. 1. Circular cylindrical shell: geometry and coordinate system.

The strain energy for a cylindrical shell, in accordance with the basic approximations of thin-shell theory, is given by [29,30]

$$U = \frac{1}{2}\int\int\int (\overline{\sigma}_x\overline{\varepsilon}_x + \overline{\sigma}_y\overline{\varepsilon}_y + \overline{\tau}_{xy}\overline{\gamma}_{xy})\,\mathrm{d}x\,\mathrm{d}y\,\mathrm{d}z \tag{1}$$

where $\overline{\varepsilon}_x$, $\overline{\varepsilon}_y$ and $\overline{\gamma}_{xy}$ are the extensional and shearing strain components at an arbitrary point of the shell, and $\overline{\sigma}_x$, $\overline{\sigma}_y$ and $\overline{\tau}_{xy}$ are the corresponding normal and shear stress components.

The generalized Hooke's law for the stress components has the form

$$\begin{Bmatrix} \overline{\sigma}_x \\ \overline{\sigma}_y \\ \overline{\tau}_{xy} \end{Bmatrix} = \begin{bmatrix} \frac{E}{(1-\nu^2)} & \frac{\nu E}{(1-\nu^2)} & 0 \\ \frac{\nu E}{(1-\nu^2)} & \frac{E}{(1-\nu^2)} & 0 \\ 0 & 0 & \frac{E}{2(1+\nu)} \end{bmatrix} \begin{Bmatrix} \overline{\varepsilon}_x \\ \overline{\varepsilon}_y \\ \overline{\gamma}_{xy} \end{Bmatrix} \tag{2}$$

The strain components at any point through the shell thickness can be written in terms of the corresponding middle surface quantities by

$$\begin{aligned} \overline{\varepsilon}_x &= \varepsilon_x + z\chi_x \\ \overline{\varepsilon}_y &= \varepsilon_y + z\chi_y \\ \overline{\gamma}_{xy} &= \gamma_{xy} + 2z\chi_{xy} \end{aligned} \tag{3}$$

where ε_x, ε_y and γ_{xy} are the extensional and shearing strain components at a point on the middle surface, z is the radial coordinate ($-h/2 \leqslant z \leqslant -h/2$) and χ_x, χ_y and χ_{xy} are, respectively, the curvature changes and twist.

Based on Donnell shallow-shell theory, the middle surface kinematic relations are given, in terms of the three displacement components by

$$\begin{aligned} &\varepsilon_x = u_{,x} + \tfrac{1}{2}w_{,x}^2 \quad \varepsilon_y = v_{,y} + \tfrac{w}{R} + \tfrac{1}{2}w_{,y}^2 \quad \gamma_{xy} = v_{,x} + u_{,y} + w_{,x}w_{,y} \\ &\chi_x = w_{,xx} \qquad\qquad \chi_y = w_{,yy} \qquad\qquad \chi_{xy} = w_{,xy} \end{aligned} \tag{4}$$

Considering both a lateral pressure p and an axial load P applied along the edges of the shell, the potential energy of the applied loads can be written as

$$V = \int\int pw\,\mathrm{d}x\,\mathrm{d}y + \oint P\,\mathrm{d}y\Big|_{x=0}^{x=L} \tag{5}$$

The kinetic energy of the shell, neglecting in-plane and rotary inertias, can be written as [30]

$$T = \frac{1}{2}\int\int\int \rho\dot{w}^2\,\mathrm{d}x\,\mathrm{d}y\,\mathrm{d}z \tag{6}$$

where $\dot{w} = \partial w/\partial t$ is the velocity in the radial direction.

The Rayleigh dissipation function is given by [31]

$$R_e = \frac{1}{2}\int\int\int 2\varepsilon\rho\omega_0\dot{w}^2\,\mathrm{d}x\,\mathrm{d}y\,\mathrm{d}z \tag{7}$$

where ε is the viscous damping coefficient and ω_0 is the lowest natural frequency of the shell.

The total energy of the non-autonomous dissipative system at any time $t>0$ is given by

$$\Pi = T + R_e - (U + V) \tag{8}$$

By applying Hamilton's principle, the nonlinear equations of motion for the cylindrical shell are given in terms of the internal forces and moments by

$$N_{x,x} + N_{xy,y} = 0 \tag{9.1}$$

$$N_{xy,x} + N_{y,y} = 0 \tag{9.2}$$

$$M_{x,xx} + 2M_{xy,xy} + M_{y,yy} + \frac{N_y}{R} + (N_x + P)w_{,xx} + N_y w_{,yy} + 2N_{xy}w_{,xy} + 2\varepsilon\rho\omega_0 h\dot{w} - p = \rho h\ddot{w} \tag{9.3}$$

where N_x, N_y and N_{xy} are in-plane normal and shearing forces intensities per unit length along the edge of a shell element and M_x, M_y and M_{xy} are the bending and twisting moment intensities, which are related to the internal stresses by the equations:

$$\begin{aligned} N_x &= \int_{-h/2}^{h/2} \overline{\sigma}_x \, dz \quad & N_y &= \int_{-h/2}^{h/2} \overline{\sigma}_y \, dz \quad & N_{xy} &= \int_{-h/2}^{h/2} \overline{\tau}_{xy} \, dz \\ M_x &= \int_{-h/2}^{h/2} z\overline{\sigma}_x \, dz \quad & M_y &= \int_{-h/2}^{h/2} z\overline{\sigma}_y \, dz \quad & M_{xy} &= \int_{-h/2}^{h/2} z\overline{\tau}_{xy} \, dz \end{aligned} \tag{10}$$

Considering a simply supported shell, the boundary conditions are

$$v(0, y) = v(L, y) = 0 \tag{11.1}$$

$$w(0, y) = w(L, y) = 0 \tag{11.2}$$

$$M_x(0, y) = M_x(L, y) = 0 \tag{11.3}$$

$$N_x(0, y) = N_x(L, y) = 0 \tag{11.4}$$

The axial force is given in terms of the displacements by

$$N_x = \frac{Eh}{1 - v^2}\left[u_{,x} + \frac{1}{2}w_{,x}^2 + v\left(v_{,y} + \frac{w}{R} + \frac{1}{2}w_{,y}^2\right)\right] \tag{12}$$

So, Eq. (11.4) constitutes a nonlinear boundary condition in terms of the displacements.

The following symmetry and continuity conditions are also used in the analysis:

$$u(L/2, y) = 0 \tag{13.1}$$

$$v(x, 0) = v(x, 2\pi R) \tag{13.2}$$

2.1. General solution of the shell displacement field by a perturbation procedure

The nonlinear equations of motion for the undamped, unforced thin shell can be written in terms of its displacement vector $\mathbf{U} = \{u, v, w\}^{\mathrm{T}}$ as

$$\mathbf{L}(\mathbf{U}) - \mathbf{U}_{,\tau\tau} = \delta\mathbf{D}_1(\mathbf{U}) + \delta^2\mathbf{D}_2(\mathbf{U}) \tag{14}$$

where $\mathbf{L}(\mathbf{U})$ is the matrix of linear differential operators, δ is an appropriate small perturbation parameter, $\mathbf{D}_1(\mathbf{U})$ is a vector of quadratic terms and $\mathbf{D}_2(\mathbf{U})$ is a vector of cubic terms.

One assumes that the components of the displacement vector $\mathbf{U}$ can be expanded in terms of the perturbation parameter δ as

$$u = \sum_{i=0}^{\infty} \delta^i u_i(x, \theta, t) \quad v = \sum_{i=0}^{\infty} \delta^i v_i(x, \theta, t) \quad w = \sum_{i=0}^{\infty} \delta^i w_i(x, \theta, t) \tag{15}$$

where δ is a small perturbation parameter.

Substituting Eq. (15) into Eq. (14), collecting terms of the same order in δ and equating these terms to zero, one obtains the following set of linear systems of partial differential equations:

$$\begin{aligned} &\mathbf{L}(\mathbf{U}^0) - \mathbf{U}^0_{,tt} = \mathbf{0} \\ &\mathbf{L}(\mathbf{U}^1) - \mathbf{U}^1_{,tt} = \mathbf{D}_1(\mathbf{U}^0) \\ &\mathbf{L}(\mathbf{U}^2) - \mathbf{U}^2_{,tt} = \mathbf{D}_1(\mathbf{U}^0, \mathbf{U}^1) + \mathbf{D}_2(\mathbf{U}^0) \end{aligned} \tag{16}$$

The solution of the first equation in Eq. (16) with the appropriate boundary conditions is simply the linear vibration modes, $\mathbf{U}^0$, and corresponding natural frequencies of the shell.

For a simply supported or infinitely long shell the vibration modes are given by

$$u_0 = \overline{U}_0 h f(t)\cos(n\theta)\cos\left(\frac{m\pi x}{L}\right)$$
$$v_0 = \overline{V}_0 h f(t)\sin(n\theta)\sin\left(\frac{m\pi x}{L}\right)$$
$$w_0 = \overline{W}_0 h f(t)\cos(n\theta)\sin\left(\frac{m\pi x}{L}\right) \tag{17}$$

where $\overline{U}_0$, $\overline{V}_0$ and $\bar{W}_0$ are the modal amplitudes, n is the number of circumferential waves, m is the number of axial half-waves in the axial direction and $\theta = y/R$.

Substitution of Eq. (17) into the second equation in Eq. (16), leads to a system of non-homogeneous differential equations, which is linear in $\mathbf{U}^1$. The particular solution of this system gives the second-order modes in the expansion Eq. (15), which are

$$u_1 = f(t)^2 h\left[\overline{U}_1\,\sin\left(\frac{2m\pi x}{L}\right) + \overline{U}_2\,\sin\left(\frac{2m\pi x}{L}\right)\cos(2n\theta)\right]$$
$$v_1 = f(t)^2 h\left[\overline{V}_1\,\sin(2n\theta) + \overline{V}_2\,\cos\left(\frac{2m\pi x}{L}\right)\sin(2n\theta)\right]$$
$$w_1 = f(t)^2 h\left[\overline{W}_1\,\cos\left(\frac{2m\pi x}{L}\right) + \overline{W}_2\,\cos(2n\theta) + \overline{W}_3\,\cos(2n\theta)\cos\left(\frac{2m\pi x}{L}\right) + \overline{W}_4\right] \tag{18}$$

These modes arise from the quadratic nonlinearity and are the main responsible for the in–out asymmetry of the shell nonlinear displacement field.

Substituting $\mathbf{U}^0$ and $\mathbf{U}^1$ in the third equation in Eq. (16), one can obtain the third-order modes $\mathbf{U}^2$. They are

$$u_2 = f(t)^3 h\left[\overline{U}_3\,\cos(n\theta)\cos\left(\frac{m\pi x}{L}\right) + \overline{U}_4\,\cos(n\theta)\left(\frac{3m\pi x}{L}\right)\right.$$
$$\left. + \overline{U}_5\,\cos(3n\theta)\cos\left(\frac{m\pi x}{L}\right) + \overline{U}_6\,\cos(3n\theta)\cos\left(\frac{3m\pi x}{L}\right)\right]$$
$$v_2 = f(t)^3 h\left[\overline{V}_3\,\sin(n\theta)\sin\left(\frac{m\pi x}{L}\right) + \overline{V}_4\,\sin(n\theta)\sin\left(\frac{3m\pi x}{L}\right)\right.$$
$$\left. + \overline{V}_5\,\sin(3n\theta)\sin\left(\frac{m\pi x}{L}\right) + \overline{V}_6\,\sin(3n\theta)\sin\left(\frac{3m\pi x}{L}\right)\right]$$
$$w_2 = f(t)^3 h\left[\overline{W}_5\,\cos(n\theta)\sin\left(\frac{m\pi x}{L}\right) + \overline{W}_6\,\cos(n\theta)\sin\left(\frac{3m\pi x}{L}\right)\right.$$
$$\left. + \overline{W}_7\,\cos(3n\theta)\sin\left(\frac{m\pi x}{L}\right) + \overline{W}_8\,\cos(3n\theta)\sin\left(\frac{3m\pi x}{L}\right)\right] \tag{19}$$

These equations have a well-defined pattern, in a way that one could continue developing higher-order modes up to the desired order without difficulty.

Finally, by inspecting the solution for $\mathbf{U}^1$, $\mathbf{U}^2$, $\mathbf{U}^3$, …, $\mathbf{U}^N$, the general solution for the displacement field can be written as

$$u = \sum_{i=1,3,5}\sum_{j=1,3,5}\overline{U}_{ij}(t)h\,\cos(in\theta)\cos\left(\frac{jm\pi x}{L}\right) + \sum_{k=0,2,4}\sum_{l=2,4}\overline{U}_{kl}(t)h\,\cos(kn\theta)\sin\left(\frac{lm\pi x}{L}\right)$$
$$v = \sum_{i=1,3,5}\sum_{j=1,3,5}\overline{V}_{ij}(t)h\,\sin(in\theta)\sin\left(\frac{jm\pi x}{L}\right) + \sum_{k=2,4,6}\sum_{l=0,2,4}\overline{V}_{kl}(t)h\,\sin(kn\theta)\cos\left(\frac{lm\pi x}{L}\right)$$
$$w = \sum_{i=1,3,5}\sum_{j=1,3,5}\overline{W}_{ij}(t)h\,\cos(in\theta)\sin\left(\frac{jm\pi x}{L}\right) + \sum_{k=0,2,4}\sum_{l=0,2,4}\overline{W}_{kl}(t)h\,\cos(kn\theta)\cos\left(\frac{lm\pi x}{L}\right) \tag{20}$$

This is the solution for an infinitely long shell, since no boundary conditions were imposed during the derivation of the higher-order modes. The powers of the perturbation parameter δ and of the function $f(t)$ are

included in the time-dependent modal amplitudes, such that

$$U^n \propto \delta^n f(t)^{n+1} + \text{higher order terms} \tag{21}$$

By imposing the out-of-plane boundary conditions Eqs. (11.2) and (11.3), the transversal displacement field of a simply supported shell can be described by

$$w = \sum_{i=1,3,5}^{\infty}\sum_{j=1,3,5}^{\infty} \zeta_{ij} h \cos(in\theta)\sin\left(\frac{jm\pi x}{L}\right) + \sum_{\alpha=0,2,4}^{\infty}\sum_{\beta=0}^{\infty} \zeta_{\alpha(2+6\beta)} h \left\{ \frac{(3+6\beta)}{(4+12\beta)}\cos(6\beta m\pi\xi) - \cos\left((2+6\beta)\frac{m\pi x}{L}\right) + \frac{(1+6\beta)}{(4+12\beta)}\cos\left((4+6\beta)\frac{m\pi x}{L}\right)\right\}\cos(\alpha n\theta) \tag{22}$$

By increasing the number of terms in Eq. (22), one can conclude that convergence can be attained up to very large deflections (around two times the shell thickness) if all modes up to the fourth order are retained in Eq. (22), i.e.,

$$\begin{aligned} w = h\Bigg[& \zeta_{11}(t)\cos(n\theta)\sin\left(\frac{m\pi x}{L}\right) + \zeta_{13}(t)\cos(n\theta)\sin\left(\frac{3m\pi x}{L}\right) + \zeta_{31}(t)\cos(3n\theta)\sin\left(\frac{m\pi x}{L}\right) \\ & + \zeta_{33}(t)\cos(3n\theta)\sin\left(\frac{3m\pi x}{L}\right) + \zeta_{02}(t)\left(\frac{3}{4} - \cos\left(\frac{2m\pi x}{L}\right) + \frac{1}{4}\cos\left(\frac{4m\pi x}{L}\right)\right) \\ & + \zeta_{22}(t)\left(\frac{3}{4} - \cos\left(\frac{2m\pi x}{L}\right) + \frac{1}{4}\cos\left(\frac{4m\pi x}{L}\right)\right)\cos(2n\theta)\Bigg] \end{aligned} \tag{23}$$

2.2. Determination of the in-plane displacements u and v

The equations of motion Eq. (9) could be solved by substituting the modal expansions derived by the perturbation procedure Eq. (20) and applying the Galerkin method as in Ref. [18]. However, the number of unknowns can be drastically reduced by obtaining analytically the in-plane displacement components u and v in terms of the modal amplitudes of w, in a procedure similar to that used in literature to obtain the stress function when Donnell equations are written in terms of the transversal displacement w and a stress function F. The number of terms in Eq. (20) to be retained for the in-plane displacement components u and v will depend on the number of terms retained in the modal expansion of w. As shown by Gonçalves and Batista [18], since u and v depend nonlinearly on w, a much larger number of terms are required to satisfy the in-plane equilibrium Eqs. (9.1) and (9.2). Here an alternative methodology is proposed to obtain the in-plane displacement components in terms of the modal amplitudes of w, satisfying exactly both the in-plane equilibrium equations and associated boundary, symmetry and continuity conditions. This constitutes the first reduction in the dimension of the system.

Consider Eq. (9.2). By substituting the in-plane forces in terms of the displacements into Eq. (9.2), one can write the partial derivative of the axial displacement $u_{,xy}$ as a function of v and w, i.e.,

$$u_{,xy} = -\frac{1}{1+v}\left[(1-v)(v_{,xx} + w_{,xx}w_{,y}) + 2\left(v_{,yy} + w_{,yy}w_{,y} + \frac{1}{R}w_{,y}\right)\right] - w_{,xy}w_{,x} \tag{24}$$

Deriving Eq. (24) twice with respect to x and twice with respect to y, one obtains respectively,

$$\begin{aligned} u_{,xxxy} = & -\frac{1}{1+v}\Bigg[(1-v)(v_{,xxxx} + w_{,xxxx}w_{,y} + 2w_{,xxx}w_{,xy} + w_{,xx}w_{xxy}) \\ & + 2\left(v_{,xxyy} + w_{,xxy}w_{,yy} + 2w_{,xy}w_{,xyy} - w_{,y}w_{,xxyy} - \frac{1}{R}w_{,xxy}\right)\Bigg] - w_{,xxx}w_{,xy} - 2w_{,xx}w_{,xxy} - w_{,x}w_{,xxxy} \end{aligned} \tag{25}$$

$$u_{,xyyy} = -\frac{1}{1+\nu}\left[(1-\nu)(v_{,xxyy} + w_{,xxyy}w_{,y} + 2w_{,xxy}w_{,yy} + w_{,xx}w_{,yyy}) + 2\left(v_{,yyyy} + 3w_{,yy}w_{,yyy} + w_{,y}w_{,yyyy} + \frac{1}{R}w_{,yyy}\right)\right] - 3w_{,xy}w_{,xyy} - w_{,x}w_{,xyyy} \tag{26}$$

Eq. (9.1) can be written in terms of the displacements as

$$2\left(u_{,xx} + w_{,x}w_{,xx} + \frac{\nu}{R}w_{,x}\right) + (1-\nu)(u_{,yy} + w_{,x}w_{,yy}) + (1+\nu)(v_{,xy} + w_{,xy}w_{,y}) = 0 \tag{27}$$

Derivation of Eq. (27) with respect to x and y and substitution of Eqs. (25) and (26) into the resulting differential equation leads to

$$\begin{aligned}\nabla^4 v = & -2w_{,xxyy}w_{,y} - w_{,xx}w_{,xxy} + \nu w_{,xx}w_{,yyy} - 2w_{,xy}w_{,xxx} \\ & - 3w_{,yy}w_{,yyy} - (2-\nu)w_{,xxy}w_{,yy} - \frac{(2+\nu)}{R}w_{,xxy} \\ & - 2(2+\nu)w_{,xy}w_{,xyy} - w_{,xxxx}w_{,y} - \frac{1}{R}w_{,yyy} - w_{,y}w_{,yyyy}\end{aligned} \tag{28}$$

where ∇^4 is the bi-harmonic operator given by

$$\nabla^4 v = v_{,xxxx} + 2v_{,xxyy} + v_{,yyyy} \tag{29}$$

By substituting the selected modal expansion for w into the right-hand side of Eq. (28), a non-homogeneous linear partial differential equation in v is obtained. The solution for the circumferential displacement may be written as $v = v_h + v_p$, where v_h is the homogeneous solution and v_p is the particular solution. The homogeneous solution is taken as zero in order to satisfy the continuity of the displacements in the circumferential direction. The particular solution can be easily obtained by substituting the expansion for w, Eq. (23), into Eq. (28) and equating the coefficients. So, the modal solution for v is obtained as a nonlinear function of the modal displacements of w. The resulting solution satisfies the boundary condition (11.1) on the average:

$$\int v(0,y)\,\mathrm{d}y = \int v(L,y)\,\mathrm{d}y = 0 \tag{30}$$

Substituting the modal solution for v and w into Eq. (25), the partial derivative of u is obtained in terms of the modal amplitudes of w. By integrating the resulting equation over the surface of the shell, one obtains:

$$\begin{aligned}u = \int\int\int\int \Bigg\{ & -\frac{1}{1+\nu}\left[(1-\nu)(v_{,xxxx} + w_{,xxxx}w_{,y} + 2w_{,xxx}w_{,xy} + w_{,xx}w_{xxy}) \right. \\ & \left. + 2\left(v_{,xxyy} + w_{,xxy}w_{,yy} + 2w_{,xy}w_{,xyy} - w_{,y}w_{,xxyy} - \frac{1}{R}w_{,xxy}\right)\right] \\ & - w_{,xxx}w_{,xy} - 2w_{,xx}w_{,xxy} - w_{,x}w_{,xxxy}\Bigg\}\,\mathrm{d}x\,\mathrm{d}x\,\mathrm{d}x\,\mathrm{d}y + F(x) + G(x,y)\end{aligned} \tag{31}$$

So, a particular solution for the axial displacement is totally defined, but for the integration functions $F(x)$ and $G(x,y)$.

By substituting Eq. (31) into Eq. (27), a non-homogeneous second-order ordinary differential equation in $F(x)$ is obtained. This equation can be written in a concise form as

$$F(x)_{,xx} = g(x) \tag{32}$$

Solving Eq. (32), one obtains:

$$F(x) = \int\int g(x)\,\mathrm{d}x\,\mathrm{d}x + C_1 x + C_2 \tag{33}$$

The integration constants C_1 and C_2 plus the function $G(x,y) = x^2 G_1(y) + xG_2(y) + G_3(y)$ are obtained by imposing the symmetry condition Eq. (13.1) and the nonlinear boundary condition Eq. (12) at $x = 0$ and L. From the two equations obtained by substituting the total displacement field into Eq. (12) and substituting

$x = 0$ and L in the resulting equation, the functions $G_1(y)$, $G_2(y)$ and C_1 are obtained ($G_1(y) = 0$). Then, from the symmetry condition Eq. (13.1), one obtains C_2 and $G_3(y)$. Finally, substituting the resulting displacement field into the original in-plane equilibrium equations and all boundary and symmetry conditions the correctness of the present procedure is demonstrated.

It is important to notice that the harmonic terms in the modal expansion for u and v derived by this procedure are similar to those derived by the perturbation procedure. However, the present methodology, by solving analytically the in-plane equilibrium equations and boundary conditions has already established the necessary number of modes in Eq. (20) and the correlation between the modal amplitudes so that the in-plane equilibrium and boundary conditions are properly satisfied.

Finally, by substituting the adopted expansion for the transversal displacement w together with the obtained expressions for u and v into the equation of motion Eq. (9.3) and by applying the standard Galerkin method, a consistent discretized system of ordinary differential equations of motion are derived.

2.3. Reduction of the problem by Karhunen–Loève decomposition

Previous works [18–20] have shown that the displacement field derived by the perturbation procedure identify all the modes that couple with the reference vibration mode through the quadratic and cubic nonlinearities present in the equations of motion and that it is capable of describing the correct softening behavior exhibited by cylindrical shells with a relatively small number of modes. It also gives some indication of the relative importance of each mode in the nonlinear solution through the powers of the small perturbation parameter. However, in order to construct a theoretically well-founded low-dimensional model, it is important to identify the relative importance of each mode to the total energy of the system as a function of the vibration amplitude and the participation of each term of the modal expansion Eq. (22) in the nonlinear vibration modes. Also, the modal basis may contain redundant information in the sense that the dynamics of the system can be approximated with accuracy by a set of functions of much lower dimension.

One way of solving this problem is to use the Karhunen–Loève method also known as POD. Various applications of the POD method for the reduced-order modeling of complex systems can be found in literature [11,13,26,32]. The POD method is based on the analysis of a series of snapshots of the system response obtained from a high-fidelity solution of the mathematical model. Experimental data have also been used to determine the snapshot sets.

In this work the snapshots are obtained from the solution of the discretized equations of motion.

A detailed mathematical formulation of the Karhunen–Loève method can be found, for example, in Bellizzi and Sampaio [33] and Sirovich [34–36]. In this work, the so-called direct method is employed [32,33].

Now consider a real vector field, $\mathbf{w}^*(\mathbf{x},\mathbf{y},t)$. This field can be decomposed into two parts: a mean time-invariant part $E[\mathbf{w}^*(\mathbf{x},\mathbf{y},t)]$. and the state variables $\mathbf{v}^*(\mathbf{x},\mathbf{y},t) = \mathbf{w}^*(\mathbf{x},\mathbf{y},t) - E[\mathbf{w}^*(\mathbf{x},\mathbf{y},t)]$, adjusted so that its mean value is zero.

In dynamic problems of mechanics, the displacement field is usually written in the space–time separated form:

$$\mathbf{v}^*(\mathbf{x},t) = \sum_{k=1}^{\infty} \xi_k(t) f_k(\mathbf{x}) \tag{34}$$

If the functions $f_k(\mathbf{x})$ and/or $\xi_k(t)$ satisfy some orthogonal and optimality properties, expansion (34) is called the POD and $f_k(\mathbf{x})$ and λ_k will be called proper orthogonal modes (POMs) and proper orthogonal values (POVs), respectively [33]. The orthogonality properties are important for the construction of reduced-order models.

The continuous displacement field at a certain instant is approximated by a discrete field. To obtain a vector field representative of the shell displacements, the surface of the shell is discretized and the displacements are evaluated at N_T spatial points uniformly spaced along the x- and y-axis, as follows:

$$\mathbf{w}^*(\mathbf{x},\mathbf{y},t) = w(x_i,y_j,t), \quad \begin{cases} x_i = iL/(n_x-1),\ i = 0,\ldots,(n_x-1) \\ y_j = j2\pi R/(n_y-1),\ j = 0,\ldots,(n_y-1) \end{cases} \tag{35}$$

where $\mathbf{w}^*(\mathbf{x},\mathbf{y},t)$ is the vector of the components of the transversal displacements measured at each point (x_i, y_j) using Eq. (23). The modal time-dependent amplitudes $\zeta_{ij}(t)$ in Eq. (23) are obtained by the solution of the discretized equations of motion of the shell. So, for each time interval a vector with $n_x \times n_y = N_T$ elements ordered as $w_1^*(t), w_2^*(t), \ldots, w_{n_T}^*(t)$ is obtained. Taking M snapshots at $t_m = m\tau$ (t_1, t_2, …, t_m), where τ is the sampling period, which must be greater than the correlation time, the following ensemble matrix of dimension $M \times N_T$ is obtained:

$$\mathbf{W}^* = \begin{bmatrix} \mathbf{w}_1 & \mathbf{w}_2 & \cdots & \mathbf{w}_{N_T} \end{bmatrix} = \begin{bmatrix} w_1(t_1) & w_2(t_1) & \ldots & w_{N_T}(t_1) \\ w_1(t_2) & w_2(t_2) & \ldots & w_{N_T}(t_2) \\ \vdots & \vdots & \ddots & \vdots \\ w_1(t_M) & w_2(t_M) & \ldots & w_{N_T}(t_M) \end{bmatrix} \tag{36}$$

where each column represents the temporal variation of the displacement at a certain point in space and each row represents the displacement field at a certain instant t_m.

Using the ergodicity hypothesis, the mean value of the field is obtained by summing all components of $\mathbf{W}^*$ and dividing the result by the number of rows M. The variation of the field with respect to the mean value of each row is obtained by

$$\mathbf{V}^* = \mathbf{W}^* - \frac{1}{M} \begin{bmatrix} \sum_{i=1}^{M} w_1(t_i) & \sum_{i=1}^{M} w_2(t_i) & \ldots & \sum_{i=1}^{M} w_{N_T}(t_i) \\ \vdots & \vdots & \ddots & \vdots \\ \sum_{i=1}^{M} w_1(t_i) & \sum_{i=1}^{M} w_2(t_i) & \ldots & \sum_{i=1}^{M} w_{N_T}(t_i) \end{bmatrix} \tag{37}$$

Finally, using again an ergodicity assumption, the spatial correlation matrix can be written as follows:

$$\mathbf{R} = \frac{1}{M}(\mathbf{V}^*)^{\mathrm{T}}(\mathbf{V}^*) \tag{38}$$

where $\mathbf{R}$ is a symmetric, positive-definite matrix.

The eigenvectors of Eq. (38), which are orthogonal due to its symmetry, are the POMs and the associated eigenvalues, the POVs. An eigenvalue (POV) has the interpretation of giving the mean energy of the system projected on the associated eigenvector-axis in function space [34–36]. The mean energy of a flow should therefore be equal to the sum of the eigenvalues.

Using the eigenvalues and eigenvectors of the spatial correlation matrix, the dynamics of the original system can be reconstructed as

$$\mathbf{w}^*(\mathbf{x},\mathbf{y},t) \approx \sum_{k=1}^{K} a_k(t)\varphi_k(\mathbf{x},\mathbf{y}) + E[\mathbf{w}^*(\mathbf{x},\mathbf{y},t)] \tag{39}$$

where $\varphi_k(\mathbf{x},\mathbf{y})$ is the kth eigenvector and $a_k(t)$ is the kth coefficient which is a function of the temporal dependence and is defined as

$$a_k(t) = \langle \mathbf{v}^*(\mathbf{x},\mathbf{y},t), \varphi_k(\mathbf{x},\mathbf{y}) \rangle \tag{40}$$

In terms of this work, the main interest is to find a set of coherent structures which captures most of the energy of the system. As a nominal criterion, we look for reduced models that capture, for example, at least 99% of the energy of the system.

3. Numerical results

Consider a cylindrical shell of radius $R = 0.2\,\mathrm{m}$, length $L = 0.4\,\mathrm{m}$ and thickness $h = 0.002\,\mathrm{m}$. The shell material has the following properties: $E = 2.1 \times 10^{11}\,\mathrm{N\,m^{-2}}$, $\nu = 0.3$ and $\rho = 7850\,\mathrm{kg\,m^{-3}}$. For this shell

geometry the lowest buckling load as well as the lowest natural frequency are obtained for $m = 1$ and $n = 5$ [20]. These values will be used throughout the present numerical analysis.

First the post-buckling analysis of the shell under axial compression is conducted. Fig. 2 shows the variation of the non-dimensional static load parameter $\Gamma_0 = P/P_{cr}$, where P is the applied load and $P_{cr} = Eh^2/[R(3-3\nu^2)^{-1/2}]$ is the classical critical load of the axially loaded shell [29], as a function of the modal amplitude ζ_{11}, considering an increasing number of modes in the modal expansions for the transversal displacement w, Eq. (23).

There is a qualitative change from hardening to softening, as already shown in previous papers [20], when the axi-symmetric mode is added to the basic vibration mode. The use of all second-order modes, which are proportional to the perturbation parameter (plus fourth-order modes due to the imposition of the out-of-plane boundary conditions) leads to a noticeable increase in the softening behavior. The addition of the third-order modes, which are proportional to the perturbation parameter squared (ζ_{13}, ζ_{31}, ζ_{33}), does not change the unstable post-buckling branch, being the corrections restricted to the large-deflection stable post-buckling branch. This is in agreement with the relative importance of each mode in terms of the perturbation parameter.

The Karhunen–Loève method is now employed to study the relative importance of each mode of the modal expansion Eq. (23) on the post-buckling response of the shell. To obtain a vector field representative of the shell deformed surface, the snapshots matrix Eq. (36) is obtained using the modal expansion Eq. (23) together with the modal coefficients ζ_{ij} obtained from the solution of the nonlinear equilibrium equation of the post-buckling response. All modes up to the fourth order in Eq. (20) are considered, which are enough to archive convergence up to very large deflections, as shown in Fig. 2. The shell surface is discretized according to Eq. (35) using $n_x = n_y = 40$. The snapshots in the Karhunen–Loève method are usually obtained as a function of time. However, it can be employed in a static nonlinear analysis treating the displacements as a function of the load parameter Γ_0 instead of t. So $\mathbf{W}^*$ in Eq. (36) is obtained for uniformly spaced steps of the applied axial load.

Fig. 3 illustrates the four first POMs and the respective POVs used in the reconstruction of the shell displacement field. They represent 99.999% of the total energy of the system. In fact, most of the energy is concentrated in the two first modes (99.89%). From these results a consistent low-dimensional model can be derived for the post-buckling analysis of the shell. Also, these results may help in identifying the relative importance of each mode in Eq. (23).

To measure the relative importance of the modes in Eq. (23) in each POM, each POM is expanded in a Fourier series, using Eq. (23). Table 1 shows the modal coefficients for each POM presented in Fig. 3. The two main contributions to the first POM, which is responsible for 96.47% of the total energy, are the basic

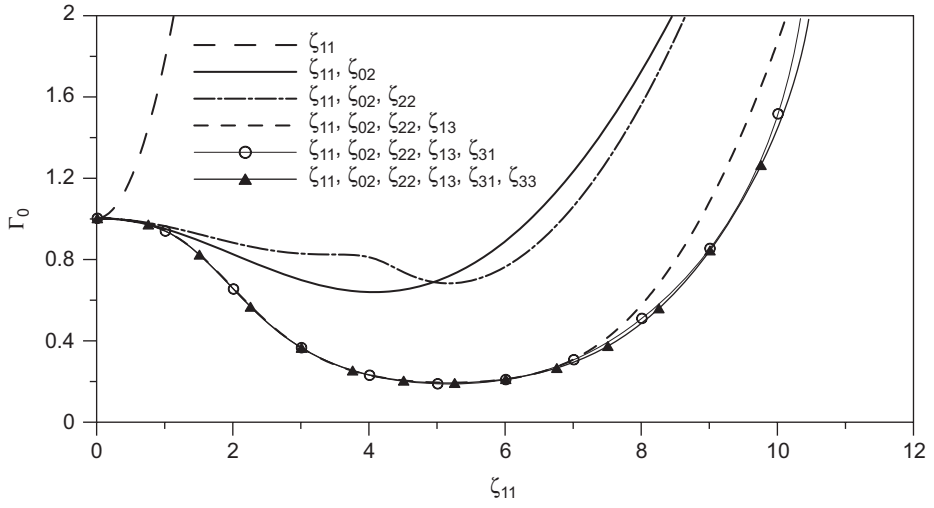

Fig. 2. Post-buckling behavior of the shell, considering different modal expansions for the transversal displacement w.

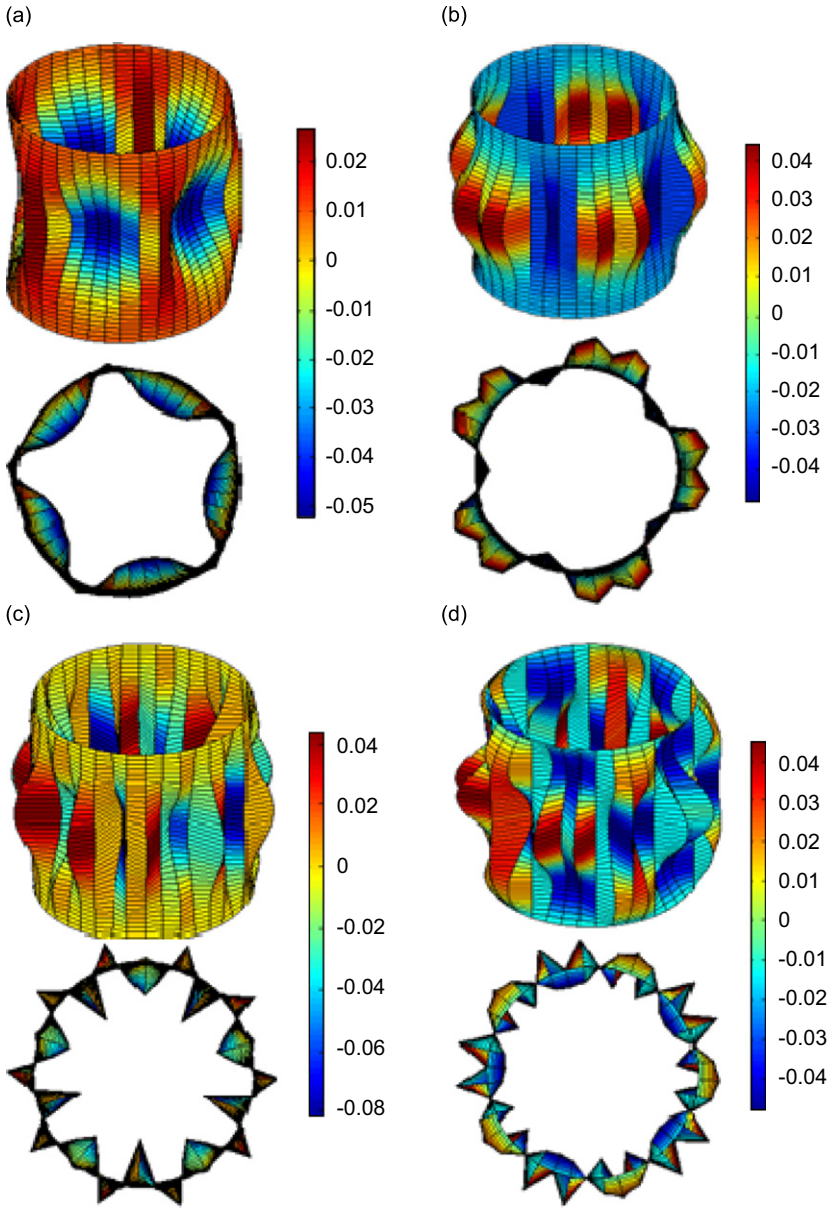

Fig. 3. The four first POMs with the respective POVs for the nonlinear post-buckling response: (a) POV = 96.47%, (b) POV = 3.42%, (c) POV = 0.10%, and (d) POV = 0.01%.

buckling mode, ζ_{11}, plus the axi-symmetric mode, ζ_{02}. This confirms the importance of these two modes, as claimed in previous works on the subject. The second POM also has significant contributions from these two modes. This explains why approximate models using only these two modes are capable of describing, at least qualitatively, the nonlinear response of the shell. The third POM is dominated by the second-order mode, ζ_{22}. The dominant amplitudes of the fourth POM are those of the third-order modes, ζ_{13}, ζ_{31} and ζ_{33}. These results agree with the solution obtained by the perturbation procedure. This analysis show that the simultaneous use of a perturbation procedure and the proper orthogonal decomposition may constitute an efficient and easily implemented procedure for the derivation of theoretically well-founded low-dimensional models.

Now, the four first POMs are used to reconstruct the response of shell. Fig. 4 shows the excellent agreement between the post-buckling response of the shell using the modal expansion (23) and using the first four modes of the Karhunen–Loève expansion.

Table 1
Participation of the modes used in the modal expansion on the first four POMs of the shell post-buckling path

POM	POV (%)	ζ_{11}	ζ_{02}	ζ_{22}	ζ_{13}	ζ_{31}	ζ_{33}
1	96.47	16.029	8.767	−3.029	−2.462	1.067	−0.455
2	3.42	17.622	−6.725	5.643	−4.271	−3.879	1.176
3	0.10	−1.592	3.194	14.537	1.437	9.631	0.503
4	0.01	4.878	−2.212	−2.888	17.025	13.139	−8.137

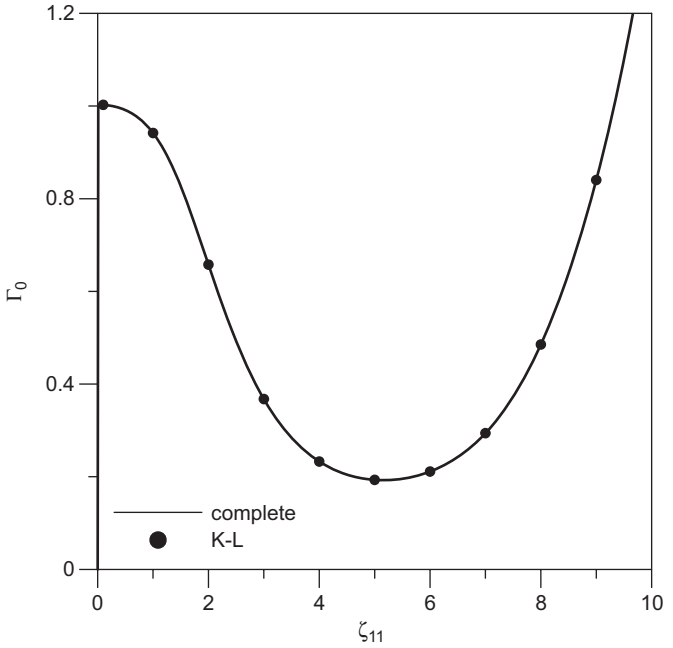

Fig. 4. Comparison of the post-buckling solution of the shell with the reconstruction of the response using the first four proper orthogonal modes.

Using the coefficients of Table 1, each POM can be described by a sum of harmonic functions with unknown amplitudes and the Galerkin method employed to deduce reduced-order models with increasing number of modes. The results are shown in Fig. 5 where the maximum normalized deflection is plotted as a function of the axial load parameter, Γ_0. Models considering two to five POMs are compared with the convergent modal solution. All models capture the softening behavior of the shell. However, the critical load is initially higher than the theoretical value but converges to the correct value as the number of POMs increases. This occurs because the first POM is not the true buckling mode of the shell but an approximation of the nonlinear buckling mode. The true mode is described by the eigenfunctions Eq. (17). It is interesting to notice that the convergence of the large-deflection post-buckling behavior is much faster.

3.1. Reduced reduced-order model

There is a basic difference between a truly multi-degree-of-freedom model with n independent coordinates and the nonlinear solution Eq. (23). Taking as a seed mode the buckling mode (m, n), all higher-order modes in Eq. (23) are due to modal coupling, as shown by the perturbation solution, leading to a modal representation of the nonlinear buckling mode. This is different from the interaction of different nonlinear

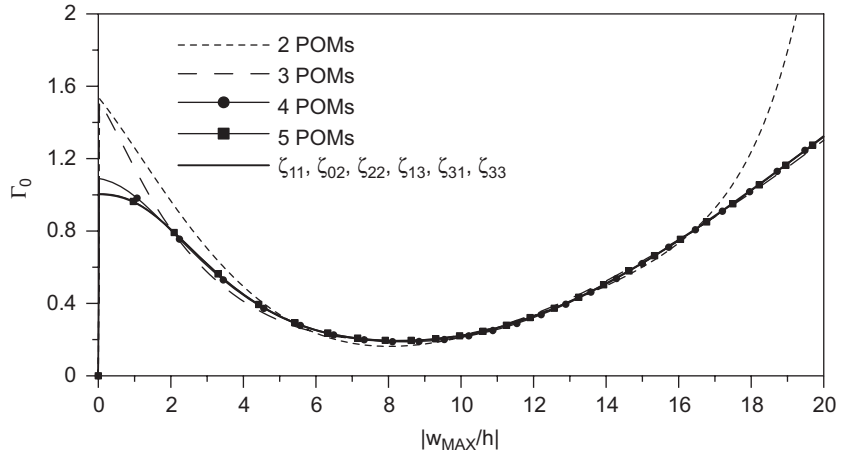

Fig. 5. Convergence of the post-buckling path using reduced-order model with increasing number of POMs.

vibration modes, as shown by Gonçalves and Del Prado [19]. So, the higher-order modal amplitudes can be viewed as slave coordinates and written as a function of ζ_{11}, i.e.

$$\begin{aligned}\zeta_{02} &= f_1(\zeta_{11})\\ \zeta_{22} &= f_2(\zeta_{11})\\ \zeta_{13} &= f_3(\zeta_{11})\\ \zeta_{31} &= f_4(\zeta_{11})\\ \zeta_{33} &= f_5(\zeta_{11})\end{aligned} \tag{41}$$

where f_i, $i = 1, \ldots, 5$, are polynomial functions of ζ_{11}.

In this way, one can construct a reduced basis from an already reduced basis based on the simultaneous use of perturbation techniques and POD. In this sense, this is a reduced reduced-order model for the shell.

To obtain the coefficients of the polynomial approximations, the modal amplitudes for increasing values of load are obtained and projected onto the $\zeta_{11} \times \zeta_{ij}$ plane and the best polynomial is obtained by the least-square method, thus minimizing the errors. For the present problem the following expansions are obtained:

$$\begin{aligned}\zeta_{02} &= 4.12 \times 10^{-2}\zeta_{11}^2 - 1.33 \times 10^{-4}\zeta_{11}^4 + 2.67 \times 10^{-6}\zeta_{11}^6\\ \zeta_{22} &= 1.54 \times 10^{-2}\zeta_{11}^2 - 7.37 \times 10^{-4}\zeta_{11}^4 + 4.05 \times 10^{-6}\zeta_{11}^6\\ \zeta_{13} &= -1.12 \times 10^{-2}\zeta_{11}^3 + 2.01 \times 10^{-4}\zeta_{11}^5 - 1.03 \times 10^{-6}\zeta_{11}^7\\ \zeta_{31} &= 3.16 \times 10^{-4}\zeta_{11}^3 - 1.72 \times 10^{-6}\zeta_{11}^5 + 1.02 \times 10^{-7}\zeta_{11}^7\\ \zeta_{33} &= 5.04 \times 10^{-4}\zeta_{11}^3 - 1.65 \times 10^{-5}\zeta_{11}^5 + 8.89 \times 10^{-8}\zeta_{11}^7\end{aligned} \tag{42}$$

In agreement with the perturbation procedure, the best fitting polynomials for ζ_{02} and ζ_{22} begins with a quadratic term in ζ_{11}^2 (see Eqs. (15.2) and (17)) and include only even powers of ζ_{11}, while the polynomials for ζ_{13}, ζ_{31} and ζ_{33} begins with a cubic term in ζ_{11} and includes only odd powers of ζ_{11} (see Eqs. (15.3) and (18)). Of course these polynomials could be derived analytically solving the systems Eq. (15), but the results would be rather cumbersome even using symbolic algebra.

Now, using Eq. (42), a single-degree-of-freedom (sdof) model is obtained for the shell. Fig. 6 shows a comparison between the complete modal solution, Eq. (23), and the reduced reduced-order model, Eq. (42). As observed, this simplified model can capture the basic nonlinear behavior of the shell up to very large amplitudes. Such a reduced-order model may find applications in several types of analysis where repeated computations are required such as in sensitivity analyses, feedback control and evolution of basins of attraction.

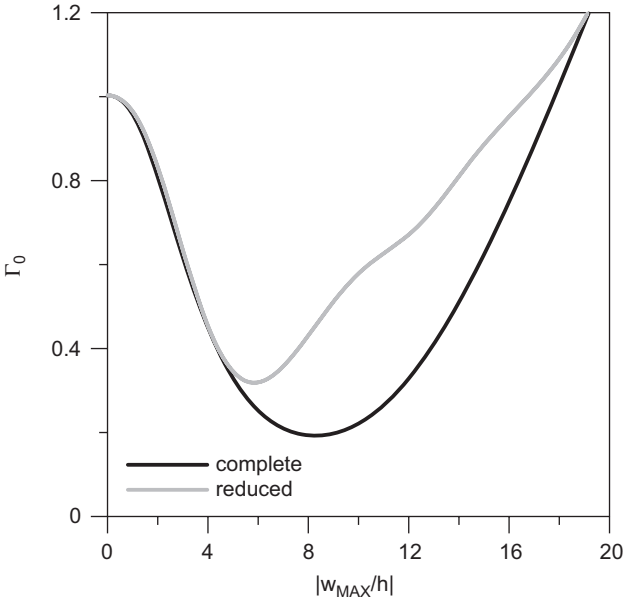

Fig. 6. Comparison of the post-buckling paths obtained using the complete modal expansion and the reduced sdof model.

3.2. Free-vibration analysis

Now a similar procedure is used to derive low-dimensional models for the nonlinear free vibrations of the shell. To obtain the frequency–amplitude relations, the discretized ordinary differential equations of motion obtained by the Galerkin method, using the modal expansion Eq. (23), are solved by the multiple shooting method to obtain periodic solutions of the initial boundary value problem [37,38]. So, no approximate functions for the time-dependent amplitudes are required. The same shell used in the static analysis is considered.

The first four POMs and the respective POVs are shown in Fig. 7. In this case, the snapshots in the Karhunen–Loève method are obtained along one period of the shell response for increasing vibration amplitudes. As in the static analysis, the first two POMs are responsible for most of the energy of the system (99.99%). Again, each POM is expanded in a Fourier series, using Eq. (23). The results are shown in Table 2. The dominant contribution of the first POM is the linear vibration mode, ζ_{11}, as expected from the theoretical foundations of Karhunen–Loève expansion. This is also the main contribution for the total energy of the shell. The second POM is basically a combination of the two second-order modes with a predominance of the axi-symmetric mode, ζ_{02}. The two first POMs are responsible for 99.99% of the total energy of the system. The third POM is dominated by the third-order mode ζ_{13}. The contributions of the other modes are negligible in this case. Again, the results are in agreement with the ones of the perturbation procedure and confirm the accuracy of approximate models used by Evensen [14] and subsequent researchers in this field.

The frequency–amplitude relation (backbone curve) obtained by the shooting method and the reconstructed response obtained by the Karhunen–Loève method are favorably compared in Fig. 8 up to large deflections (two times the shell thickness). The backbone curve exhibits, as expected, a softening behavior. The softening behavior exhibited by most cylindrical shell geometries are due mainly to the modal coupling between the linear vibration mode and the second-order modes given by Eq. (18), leading to a strong negative quadratic term in the discretized reduced model [18–20]. The degree of softening may very slightly, depending on the adopted shell theory and discretization procedure.

Fig. 9 shows the variation of each modal coordinate along a period of the free-vibration response and the results obtained by the reconstruction of the response using the orthogonal basis for $\Omega = 0.98$ and the following set of initial conditions $\zeta_{11(0)} = 1.0$, $\zeta_{02}(0) = 0.038$, $\zeta_{22}(0) = 0.013$, $\zeta_{13}(0) = -0.021$, $\zeta_{31}(0) = 0.0007$,

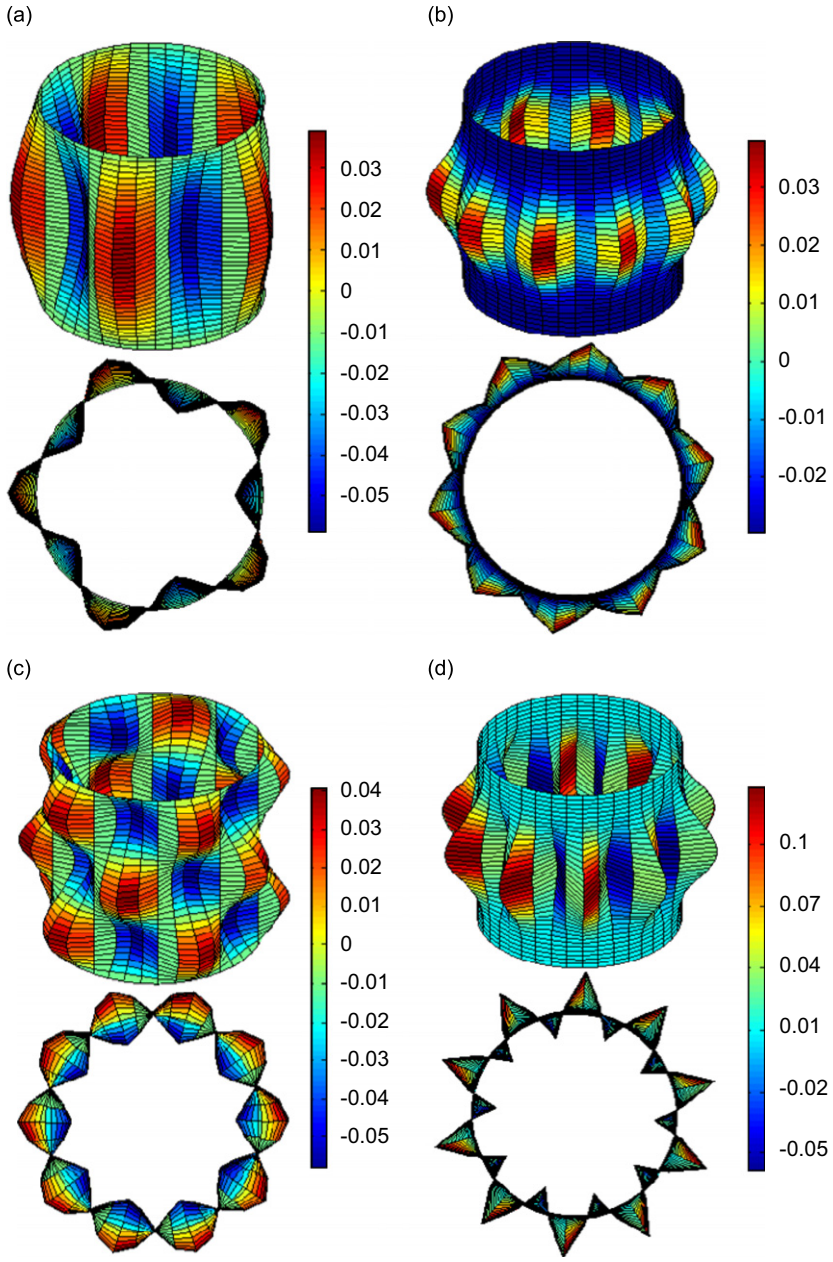

Fig. 7. The four first POMs and the respective POVs for the nonlinear free-vibration response: (a) POV = 99.80%, (b) POV = 0.19%, (c) POV = 0.007% and (d) POV = 0.0001%.

Table 2
Participation of the modes used in the modal expansion on the first four POMs of the shell frequency–amplitude relation (backbone curve)

POM	POV (%)	$\zeta_{11}(t)$	$\zeta_{02}(t)$	$\zeta_{22}(t)$	$\zeta_{13}(t)$	$\zeta_{31}(t)$	$\zeta_{33}(t)$
1	99.80	−24.395	−0.00011	−0.00001	0.282	−0.011	−0.003
2	0.19	−1.075	−10.997	−5.541	0.003	−0.0001	0.00006
3	0.007	0.298	−0.224	−0.102	24.374	−0.773	0.270
4	0.0001	0.726	−4.323	15.566	−0.350	0.012	−0.004

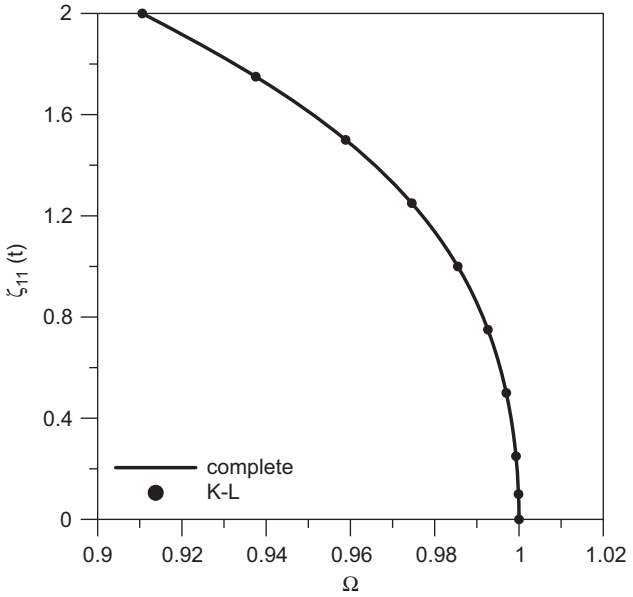

Fig. 8. Frequency–amplitude relation for the simply supported cylindrical shell using the modal expansion obtained by the perturbation procedure and the K–L expansion.

$\zeta_{33}(0) = -0.0002$, $\dot{\zeta}_{11}(0) = \dot{\zeta}_{02}(0) = \dot{\zeta}_{22}(0) = \dot{\zeta}_{13}(0) = \dot{\zeta}_{31}(0) = \dot{\zeta}_{33}(0) = 0.0$. These initial conditions are cinematically consistent since they are the result of the multiple shooting method for $\Omega = 0.98$. Again, an excellent agreement is observed. The numerically obtained variation of the second- and third-order coordinates along one period are in agreement with the powers of the time function of the linear vibration mode $f(t)$ in Eq. (20).

The frequency–amplitude relation (backbone curve) obtained by the Galerkin method using two and three POMs are compared with the convergent solution in Fig. 10. As expected, the use of the first two POMs, including basically, as shown in Table 2, the contributions of the linear vibration and axi-symmetric mode already describes the general nonlinear behavior of the shell. The inclusion of the third POM lead to a precise solution up to very large deflections (two times the shell thickness).

3.3. Reduced reduced-order model for free-vibration analysis

For the frequency–amplitude relation, the slave coordinates can be approximated by the following polynomial expansions of the seed coordinate $\zeta_{11}(t)$:

$$\begin{aligned}
\zeta_{02}(t) &= 3.78 \times 10^{-2}\zeta_{11}^2(t) + 8.82 \times 10^{-4}\zeta_{11}^4(t) + 3.38 \times 10^{-5}\zeta_{11}^6(t)\\
\zeta_{22}(t) &= 8.89 \times 10^{-3}\zeta_{11}^2(t) + 5.19 \times 10^{-4}\zeta_{11}^4(t) - 6.92 \times 10^{-4}\zeta_{11}^6(t)\\
\zeta_{13}(t) &= -2.17 \times 10^{-2}\zeta_{11}^3(t) + 1.11 \times 10^{-3}\zeta_{11}^5(t) - 2.56 \times 10^{-4}\zeta_{11}^7(t)\\
\zeta_{31}(t) &= 4.99 \times 10^{-4}\zeta_{11}^3(t) + 2.58 \times 10^{-4}\zeta_{11}^5(t) - 4.56 \times 10^{-5}\zeta_{11}^7(t)\\
\zeta_{33}(t) &= -2.33 \times 10^{-5}\zeta_{11}^3(t) - 2.45 \times 10^{-4}\zeta_{11}^5(t) + 4.27 \times 10^{-5}\zeta_{11}^7(t)
\end{aligned} \tag{43}$$

As in the static case, the best fitting polynomials are in agreement with the perturbation procedure.

Based on expressions Eq. (43) a reduced sdof model is obtained and the frequency–amplitude relation derived from this model is compared with the response of the complete model in Fig. 11. This reduced reduced-order model can capture the type and degree of nonlinearity of the shell up to large deflections.

It is expected that a properly derived reduced-order model will work in an interpolatory setting, but it is not clear what happens in an extrapolatory setting. One cannot hope to determine one reduced-order model capable of describing the response of a complex system for all sets of parameters. So, depending on the

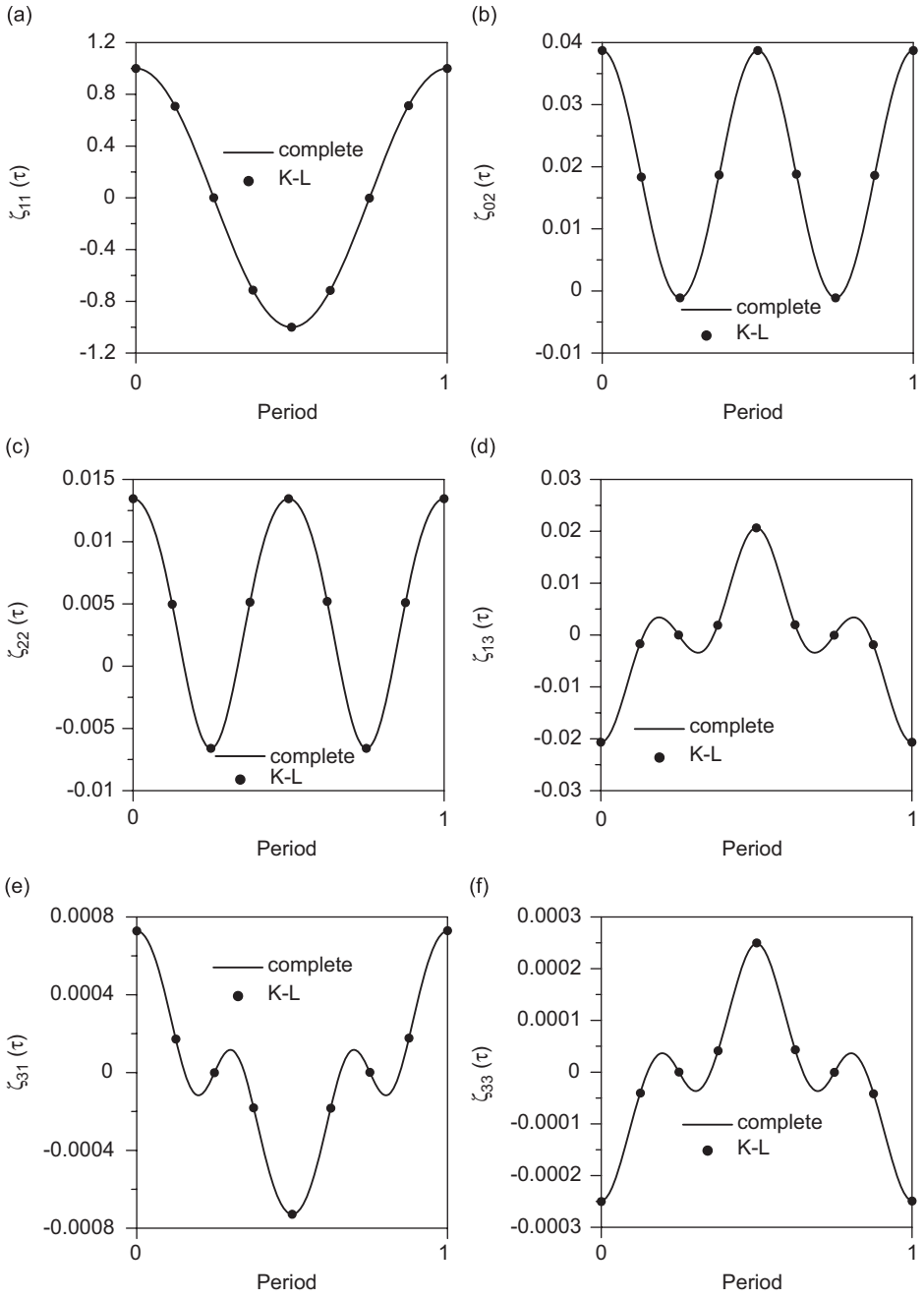

Fig. 9. Variation of each modal amplitude along a period of the free-vibration response.

complexity of the systems, various reduced-order models optimized for different sets of parameters should be derived. However, one hopes that a single reduced basis can be used for several state simulations or in several design settings. So, its is expected that the derived reduced models for free-vibration analysis will also give reliable results in the forced vibration analysis of the shell, since it captures the main nonlinearities of the problem. Although a detailed forced vibration analysis is beyond the scope of the present work, a brief study of the forced response of a shell under lateral harmonic pressure is undertaken to verify the quality of the reduced models.

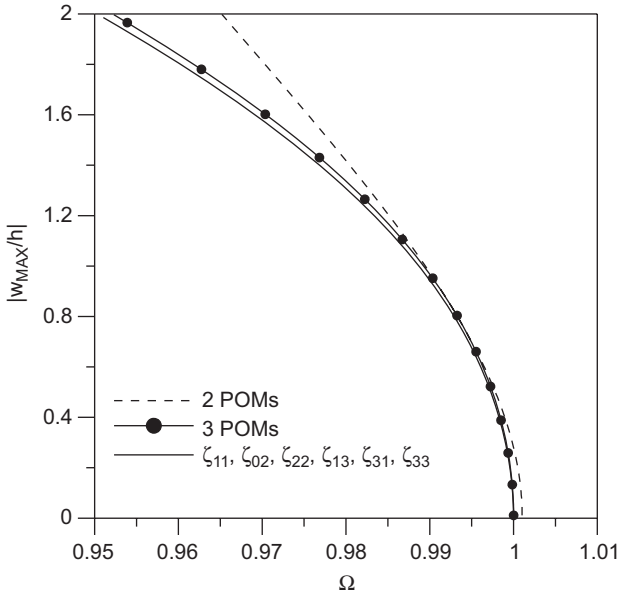

Fig. 10. Comparison of reduced-order models using two and three POMs with the convergent modal solution.

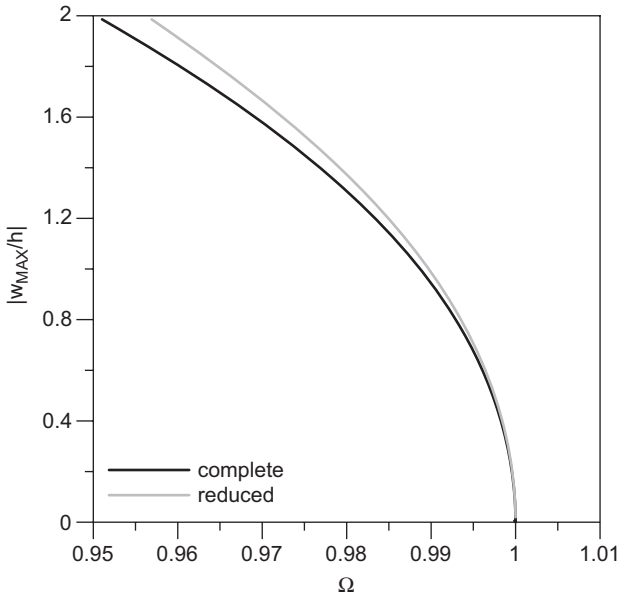

Fig. 11. Frequency–amplitude relation obtained by the complete modal solution and the sdof model (reduced reduced-order model).

The lateral pressure has the following distribution:

$$p = \overline{P}h\,\cos(n\theta)\sin\left(\frac{m\pi x}{L}\right) \tag{44}$$

where $\overline{P}$ is the time-dependent amplitude in $\mathrm{kN\,m^{-2}}$.

In Fig. 12 the maximum radial deflection of the shell is plotted as a function of the forcing frequency for selected values of the forcing magnitude parameter, $\Gamma_1 = \overline{P}/P_{\mathrm{cr}}$, where P_{cr} is the critical load of the shell under

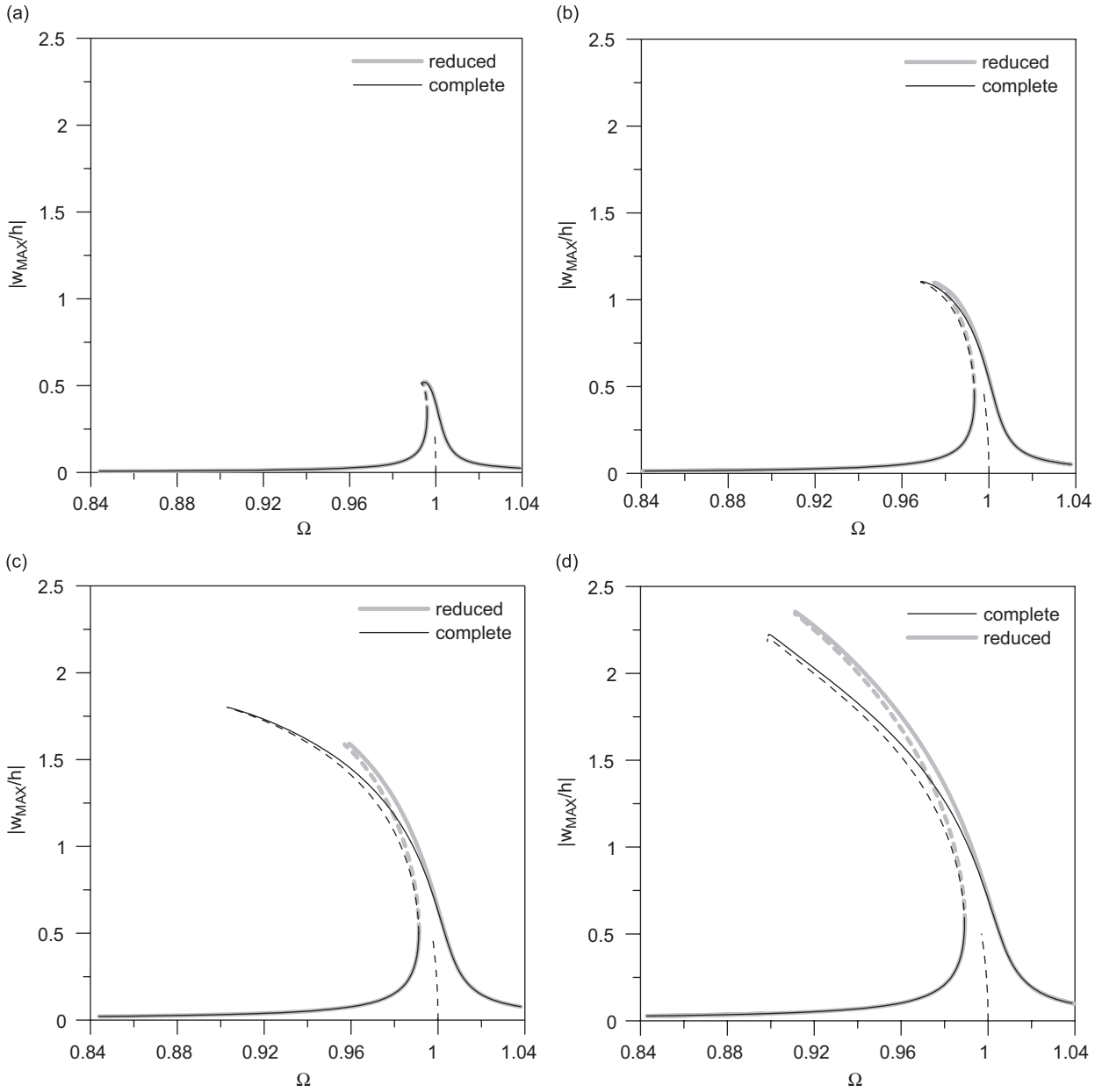

Fig. 12. Frequency–response curves (maximum lateral deflection versus excitation frequency) for increasing values of the magnitude of the external lateral pressure, Γ_1. $\varepsilon = 0.001$. Solid line: stable. Dashed line: unstable. (a) $\Gamma_1 = 0.25$, (b) $\Gamma_1 = 0.50$, (c) $\Gamma_1 = 0.75$, and (d) $\Gamma_1 = 1.00$.

lateral pressure, which is given by [29]

$$P_{\mathrm{cr}} = \frac{Eh}{R}\left[\frac{[(\pi R/L)^2 + n^2]^2}{n^2}\,\frac{(h/R)^2}{12(1-\nu^2)} + \frac{(\pi R/L)^4}{n^2[(\pi R/L)^2 + n^2]^2}\right] \tag{45}$$

These resonance curves were obtained using continuation techniques for the complete model and the reduced-order sdof model deduced previously. The two solutions agree quite well for vibration amplitudes less than two times the shell thickness and load level lower than the static critical load. The results are obtained

considering a damping coefficient $\varepsilon = 0.001$. Considering the extreme case of $\Gamma_1 = 1.0$, Fig. 13 shows the response for two different damping rations. Again a good comparison is observed.

In the forced vibration analysis of the perfect shell, the influence of the companion mode participation is neglected. Amabili et al. [25,26] already studied POD reduction considering companion mode participation. Their results show that the companion mode has an important influence on the response in the resonance region. The present reduction procedure, based on a perturbation procedure and POD, can also be employed considering the presence of the companion mode in the modal expansion.

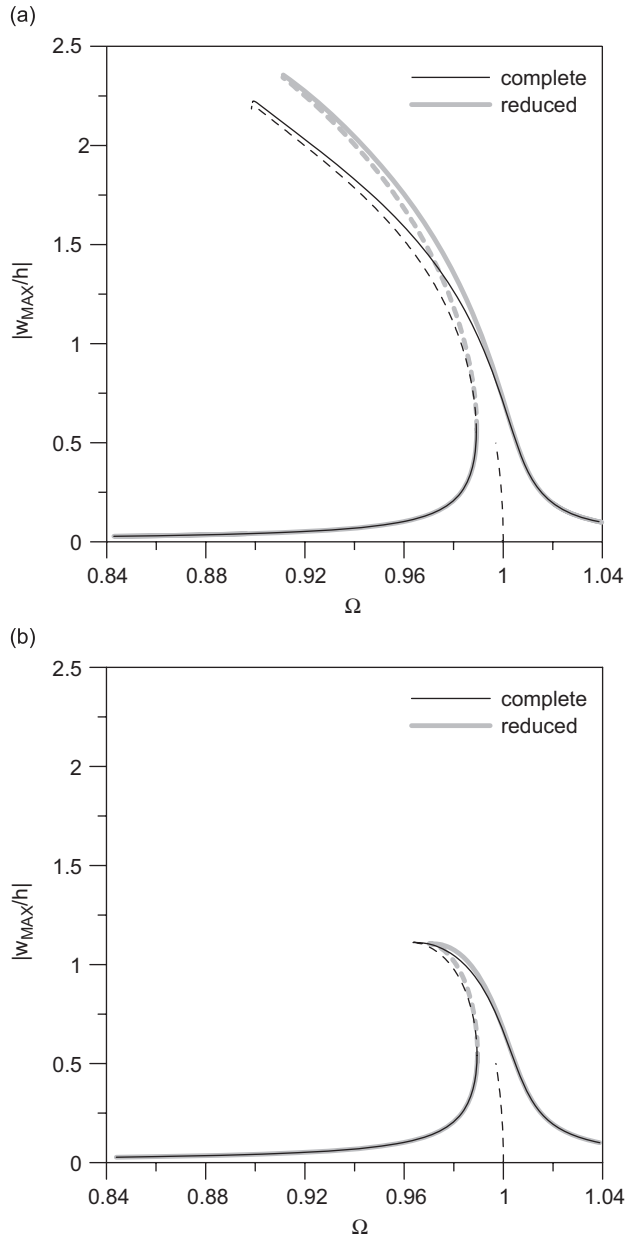

Fig. 13. Frequency–response curves (maximum lateral deflection versus excitation frequency) for $\Gamma_1 = 1.0$ and two different values of the damping ratio, ε. Solid line: stable. Dashed line: unstable. (a) $\varepsilon = 0.001$ and (b) $\varepsilon = 0.002$.

4. Conclusions

In this work, the construction of low-dimensional models for the nonlinear buckling and vibration analysis of thin-walled cylindrical shell using both a perturbation procedure and proper orthogonal decomposition is discussed in detail. First a consistent series solution, based on the perturbation procedure, which satisfy the out-of-plane boundary conditions of a simply supported shell is proposed. Based on this solution, an alternative methodology is presented to solve analytically the in-plane equilibrium equations together with the corresponding boundary, symmetry and continuity conditions. In this way the in-plane displacements are written as a function of the out-of-plane modal amplitudes, reducing considerably the number of unknowns of the discretized system. It is shown that this leads to an efficient modal solution that can archive convergence up to large deflections, around two times the shell thickness, with a relatively small number of modes. Then using this modal solution, the proper orthogonal modes and respective proper orthogonal values are derived to study the influence of each mode of the modal solution on the response and total energy of the system. The results show excellent agreement with the ones obtained by the perturbation procedure and clarify the influence of the modal couplings on the nonlinearity of the shell. Using the concept of slave coordinates a reduced reduced-order model with one degree of freedom is derived. This model captures the degree and type of nonlinearity of the shell and compare well with the more refined models. Finally, these models are used to study the nonlinear forced response of the shell under harmonic lateral forcing. The present procedure, combining a perturbation procedure with POD, can be easily extended to a series of structural elements such as beams, arches and plates and other shell geometries. Once the linear vibration modes are obtained, the higher-order nonlinear modes can be derived by the perturbation procedure and, then, the POD method can be used to select the most important modes. It leads, as shown by the present results, to consistent low-dimensional models which can be effectively used in time-consuming procedures such as continuation or homotopy methods for computing state solutions, in particular bifurcation diagrams under dynamic loads, evolution and erosion of basins of attraction, feedback control, parametric studies of state solutions and identification of stability boundaries in control space.

Acknowledgments

The authors are grateful for the financial support from the Brazilian National Council for Scientific and Technological Development (CNPq/MCT) and the Carlos Chagas Filho Foundation (FAPERJ/CNE).

References

[1] H.N. Chu, Influence of large amplitudes on flexural vibrations of a thin circular cylindrical shells, *Journal of Aerospace Science* 28 (1961) 302–609.
[2] D.A. Evensen, Some observations on the nonlinear vibration of thin cylindrical shells, *AIAA Journal* 1 (1963) 2857–2858.
[3] E.H. Dowell, C.S. Ventres, Modal equations for the nonlinear flexural vibrations of a cylindrical shells, *International Journal of Solids and Structures* 4 (1968) 2857–2858.
[4] S. Atluri, A perturbation analysis of nonlinear free flexural vibrations of a circular cylindrical shell, *International Journal of Solids and Structures* 8 (1972) 549–569.
[5] J.C. Chen, C.D. Babcock, Nonlinear vibration of cylindrical shells, *AIAA Journal* 13 (1975) 868–876.
[6] J.H. Ginsberg, Propagation of nonlinear acoustic waves induced by a vibrating cylinder, *Journal of the Acoustic Society of America* 64 (1978) 1671–1687.
[7] M. Amabili, M.P. Païdoussis, Review of studies on geometrically nonlinear vibrations and dynamics of circular cylindrical shells and panels, with and without fluid–structure interaction, *Applied Mechanics Reviews* 56 (2003) 655–699.
[8] V.D. Kubenko, P.S. Koval'chuk, Nonlinear problems of the vibration of thin shells (review), *International Applied Mechanics* 34 (1998) 703–728.
[9] S.W. Shaw, C. Pierre, Normal modes for nonlinear vibratory systems, *Journal of Sound and Vibration* 164 (1) (1993) 85–124.
[10] A.H. Nayfeh, *Method of Normal Forms*, Wiley, New York, 1993.
[11] A. Steindl, H. Troger, Methods for dimension reduction and their applications in nonlinear dynamics, *International Journal of Solids and Structures* 38 (2001) 2131–2147.
[12] J. Burkardt, M. Gunzburger, H. Lee, Centroidal Voronoi tessellation-based reduced-order modeling of complex systems, *SIAM Journal on Scientific Computing* 28 (2) (2006) 459–484.
[13] G. Rega, H. Troger, Dimension reduction of dynamical systems: methods, models, applications, *Nonlinear Dynamics* 41 (2005) 1–15.

[14] D.A. Evensen, Nonlinear flexural vibrations of thin-walled circular cylinders, *NASA TN* D-4090, 1967.
[15] M.D. Olson, Some experimental observations on the nonlinear vibrations of cylindrical shells, *AIAA Journal* 3 (1965) 1775–1777.
[16] J.G.A. Croll, R.C. Batista, Explicit lower bounds for the buckling of axially loaded cylinders, *International Journal of Mechanical Sciences* 23 (1981) 331–343.
[17] G.W. Hunt, K.A.J. Williams, R.G. Cowell, Hidden symmetry concepts in the elastic buckling of axially-loaded cylinders, *International Journal of Solids and Structures* 22 (1986) 1501–1515.
[18] P.B. Gonçalves, R.C. Batista, Nonlinear vibration analysis of fluid-filled cylindrical shells, *Journal of Sound and Vibration* 127 (1988) 133–143.
[19] P.B. Gonçalves, Z.J.G.N. Del Prado, Effect of nonlinear modal interaction on the dynamic instability of axially excited cylindrical shells, *Computers and Structures* 82 (2004) 2621–2634.
[20] P.B. Gonçalves, Z.J.G.N. Del Prado, Low-dimensional Galerkin models for nonlinear vibration and instability analysis of cylindrical shells, *Nonlinear Dynamics* 41 (2005) 129–145.
[21] M. Amabili, F. Pellicano, M.P. Païdoussis, Nonlinear dynamics and stability of circular cylindrical shells containing flowing fluid. Part I: stability, *Journal of Sound and Vibration* 225 (1999) 655–699.
[22] M. Amabili, Theory and experiments for large-amplitude vibrations of empty and fluid-filled circular cylindrical shells with imperfections, *Journal of Sound and Vibration* 262 (4) (2003) 921–975.
[23] A.A. Popov, Auto-parametric resonance in thin cylindrical shells using the slow fluctuation method, *Thin-Walled Structures* 42 (2004) 475–495.
[24] E.L. Jansen, Dynamic stability problems of anisotropic cylindrical shells via a simplified analysis, *Nonlinear Dynamics* 39 (2005) 349–367.
[25] M. Amabili, A. Sarkar, M.P. Païdoussis, Reduced-order models for nonlinear vibrations of cylindrical shells via the proper orthogonal decomposition method, *Journal of Fluids and Structures* 18 (2003) 227–250.
[26] M. Amabili, A. Sarkar, M.P. Païdoussis, Chaotic vibrations of circular cylindrical shells: Galerkin versus reduced-order models via the proper orthogonal decomposition method, *Journal of Sound and Vibration* 290 (2006) 736–762.
[27] M. Amabili, C. Touzé, Reduced-order models for nonlinear vibrations of fluid-filled circular cylindrical shells: Comparison of POD and asymptotic nonlinear normal modes methods, *Journal of Fluids and Structures* 23 (2007) 885–903.
[28] C. Touzé, M. Amabili, Nonlinear normal modes for damped geometrically nonlinear systems: application to reduced-order modeling of harmonically forced structures, *Journal of Sound and Vibration* 298 (2006) 958–981.
[29] D.O. Brush, B.O. Almroth, *Buckling of Bars, Plates and Shells*, McGraw-Hill, New York, 1975.
[30] H. Kraus, *Thin Elastic Shells*, Wiley, New York, 1967.
[31] A.A. Popov, J.M.T. Thompson, F.A. McRobie, Low dimensional models of shell vibration: parametrically excited vibrations of cylindrical shells, *Journal of Sound and Vibration* 209 (1998) 163–186.
[32] C. Wolter, An Introduction to Model Reduction Based on Karhunen–Loève Expansions, MSc Dissertation, Catholic University of Rio de Janeiro, PUC-Rio, Rio de Janeiro, Brazil, 2001.
[33] S. Bellizzi, R. Sampaio, POMs analysis of randomly vibrating systems obtained from Karhunen–Loève expansion, *Journal of Sound and Vibration* 297 (2006) 774–793.
[34] L. Sirovich, Turbulence and the dynamics of coherent structures, part I: coherent structures, *Quarterly of Applied Mathematics* 45 (1987) 561–571.
[35] L. Sirovich, Turbulence and the dynamics of coherent structures, part II: symmetries and transformations, *Quarterly of Applied Mathematics* 45 (1987) 573–582.
[36] L. Sirovich, Turbulence and the dynamics of coherent structures, part III: dynamics and scaling, *Quarterly of Applied Mathematics* 45 (1987) 583–590.
[37] R. Seydel, *From Equilibrium to Chaos: Practical Bifurcation and Stability Analysis*, Elsevier, Amsterdam, 1988.
[38] D. Li, J. Xu, A new method to determine the periodic orbit of nonlinear dynamic system and its period, *Engineering with Computers* 20 (2005) 316–322.